Application of Unscented Kalman Filter for Condition Monitoring of an Organic Rankine Cycle Turbogenerator

Leonardo Pierobon[1], Rune Schlanbusch[2], Rambabu Kandepu[3] and Fredrik Haglind[4]

[1,4] *Department of Mechanical Engineering, Technical University of Denmark*
Building 403, 2800 Kongens Lyngby, Denmark
lpier@mek.dtu.dk
frh@mek.dtu.dk

[2,3] *Teknova AS*
Gimlemoen 19, 4630 Kristiansand, Norway
Rune.Schlanbusch@teknova.no
Rambabu.Kandepu@teknova.no

ABSTRACT

This work relates to a project focusing on energy optimization on offshore facilities. On oil and gas platforms it is common practice to employ gas turbines for power production. So as to increase the system performance and reduce emissions, a bottoming cycle unit can be designed with particular emphasis on compactness and reliability. In such context, organic Rankine cycle turbogenerators are a promising technology. The implementation of an organic Rankine cycle unit is thus considered for the power system of the Draugen offshore platform in the northern sea, which is the case study for this project. Considering the plant dynamics, it is of paramount importance to monitor the peak temperatures within the once-through boiler serving the bottoming unit to prevent the decomposition of the working fluid. This paper accordingly aims at applying the unscented Kalman filter to estimate the temperature distribution inside the primary heat exchanger by engaging a detailed and distributed model of the system and available measurements. Simulation results prove the robustness of the unscented Kalman filter with respect to process noise, measurement disturbances and initial conditions.

1. INTRODUCTION

Owing to environmental concerns and with increasing incentives for reducing CO_2 emissions and pollutants offshore, optimization of energy usage on oil and gas facilities has become a focus area. On offshore platforms one or more redundant gas turbines supply the electric power demand. As an example, a standard operational strategy is to share the load between two engines, while a third is on stand-by or on maintenance. The two gas turbines typically run at fairly low loads (around 50%) in order to decrease the risk of failure of the system, which would cause a high economic loss to the platform operator. On the other hand, this operational strategy reduces significantly the system performance, which in turns results in a large amount of waste heat contained in the exhaust gases exiting the engines (Nguyen et al., 2013).

A viable solution to enhance the efficiency is to implement a waste heat recovery unit at the bottom of the gas turbines. A mature technology accomplishing this duty is the Steam Rankine Cycle (SRC) power module. (Kloster, 1999) described the existing SRC units in the Oseberg, Eldfisk and Snorre B offshore installations. Air Bottoming Cycles (ABCs) constitute a valid alternative to SRC units as they employ a non-toxic and inflammable working fluid. Moreover, ABC power modules do not require a condenser as they operate as open-cycles, thus leading to high compactness and low weight. (Bolland, Forde, & Hånde, 1996) carried out a feasibility study on the implementation of ABCs offshore. Results proved that, despite the low gain in performance, low weight and short pay-back time can be achieved. (Pierobon, Nguyen, Larsen, Haglind, & Elmegaard, 2013) proposed instead the use of Organic Rankine Cycle (ORC) power modules by tailoring their design to the Draugen oil and gas facility. For the same case study, (Pierobon, Haglind, Kandepu, Fermi, & Rossetti, 2013) demonstrated that the use of ORC units provides larger economic revenues and power system performances compared to ABC and SRC modules.

While ORC turbogenerators work in principle similarly to steam Rankine cycle units, the working fluid is instead an

organic compound characterized by lower critical temperatures and pressures than water, thus making these systems suitable for low and medium temperature waste heat recovery (Quoilin, Broek, Declaye, Dewallef, & Lemort, 2013). As a drawback, organic fluids may experience chemical deterioration and decomposition at high temperatures. This criticality is owed to the breakage of chemical bonds between the molecules and the formation of smaller compounds, which can then react to create other hydrocarbons. As the system performance strongly relates to transport and physical properties of the working fluid, those chemical phenomena can severely reduce the net power output and the components' lifetime. In such context, monitoring the temperature profiles inside the heat exchangers serving the ORC unit is a pivotal aspect to enhance plant reliability and reduce maintenance periods.

A possible solution accomplishing these tasks is the Kalman Filter (KF), an algorithm which employs a state space model of the system and measurements ascertained over time, containing noise and disturbances, and provides estimates of unknown variables that are usually more accurate than those based on a single measurement alone. As examples of applications to heat exchangers, (G. Jonsson & Palsson, 1994) used the KF algorithm to adjust generic empirical correlations commonly employed to estimate the heat transfer coefficients, while (Loparo, Buchner, & Vasudeva, 1991) proposed a non-linear KF algorithm for leak detection in an experimental laboratory heat exchanger process. More recently, (G. R. Jonsson, Lalot, Palsson, & Desmet, 2007) demonstrated the use of an Extended Kalman Filter (EKF) to detect fouling in heat exchangers.

Notwithstanding the aforementioned works, to the knowledge of the authors the KF algorithm has not yet been applied to ORC waste heat recovery systems. This paper accordingly aims at demonstrating the use of the Kalman filter to estimate the temperature distribution in the primary heat exchanger of an ORC unit, which is used to augment the performance of the gas turbine-based power system installed on the Draugen oil and gas platform. It is reported that Unscented Kalman Filter (UKF) performs better in estimating the state variables in a non-linear system in comparison with EKF (Kandepu, Foss, & Imsland, 2008). Accordingly in this article, the UKF is applied to the ORC unit with focus on the primary heat exchanger. A state space model of the ORC system based on first principles is developed. Disturbances are assumed for measurements of temperature, mass flow and density utilizing in-silico simulation-based data and assuming a Gaussian distribution. The UKF is thus applied to estimate the temperature distribution inside the main heat exchanger while the remaining variables are assumed to be measurable.

This paper is structured as follows: Section 2 introduces the case study, and Section 3 describes the state space model of the ORC turbogenerator. The unscented Kalman filter algorithm is then outlined in Section 4, while the results are reported and discussed in Section 5. Concluding remarks are given in Section 6.

2. CASE STUDY

The case study is the power system installed on the Draugen oil and gas offshore platform, located 150 km from Kristiansund, in the Norwegian Sea. The reservoir was discovered in 1984 and started operation in 1993. The platform, operated by A/S Norske Shell, produces gas exported via Åsgard gas pipeline to Kårstø (Norway) and oil, which is first stored in tanks at the bottom of the sea and then exported via a shuttle tanker (once every 1-2 weeks). The normal power demand is around 19 MW and it can increase up to 25 MW during oil export. To enhance the reliability and to diminish the risk of failure of the power system, two turbines run at a time covering 50% of the load each, while the third one is kept on standby, allowing for maintenance work. Despite the low performance, this strategy ensures the necessary reserve power for peak loads, and the safe operation of the engines.

Figure 1 shows the layout of the power system with the additional ORC turbogenerator recovering the heat contained in the exhaust gases produced by gas turbine A. Gas turbines B and C are not reported. Note that the bottoming cycle units should have the capability to harvest the waste heat alternatively from the other two engines, thus ensuring high performances when switching the gas turbines on operation. The twin-spool engine employs two coaxial shafts coupling the Low Pressure Compressor (LPC) with the Low Pressure Turbine (LPT) and the High Pressure Compressor (HPC) with the High Pressure Turbine (HPT). The Power Turbine (PT) transfers mechanical power through a dedicated shaft to the electric Generator (GEN). Natural gas is the fuel utilized in the Combustion Chamber (CC).

The ORC unit comprehends the single-pressure non-reheat Once-Through Boiler (OTB), the turbine, the sea-water cooled shell-and-tube condenser and the feed-water pump. The working fluid is cyclopentane (C_5H_{10}), a compound widely adopted for operating ORC systems in this range of temperature, see e.g. (Del Turco et al., 2011). As the slope of the saturation curve of cyclopentane is positive (dry fluid), a shell-and-tube recuperator is added to decrease the energy contained in the superheated vapour exiting the ORC expander. Figure 2 illustrates the $T - s$ diagrams of the ORC power unit considered in this study. Starting from point 3, cyclopentane is first preheated ($3 \rightarrow 4$), vaporized ($4 \rightarrow 5$) and superheated ($5 \rightarrow 6$) in the once-through boiler. The fluid is then expanded in the turbine ($6 \rightarrow 7$) , and cooled down in the recuperator ($7 \rightarrow 8$). In this manner the inlet temperature in the OTB can be enhanced by recovering energy from the superheated vapour exiting the turbine. The working fluid is

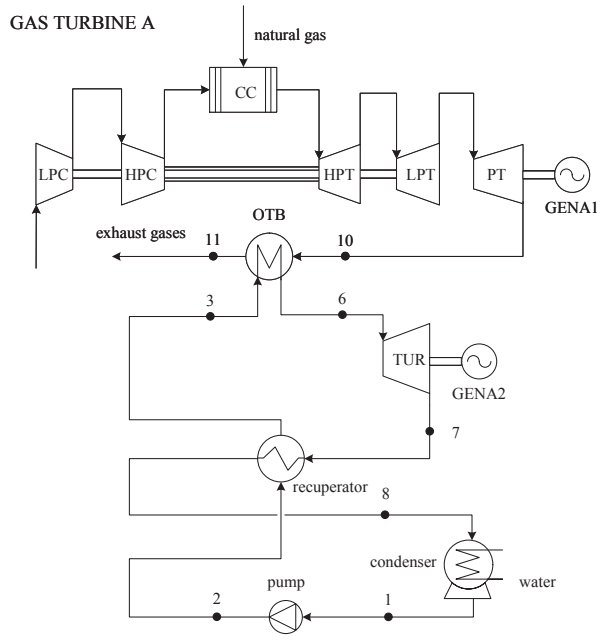

Figure 1. Simplified layout of the power system on the Draugen offshore oil and gas platform. Gas turbine B and C are not shown. The organic Rankine cycle module recuperates part of the thermal power released with the exhaust gases of one engine, in the case gas turbine A.

then condensed ($8 \rightarrow 9 \rightarrow 1$) and pumped up ($1 \rightarrow 2$) to the highest pressure level through the cold side of the recuperator ($2 \rightarrow 3$), thus closing the cycle. Note that Figure 1 does not report node 9 as the saturated vapour condition occurs inside the condenser.

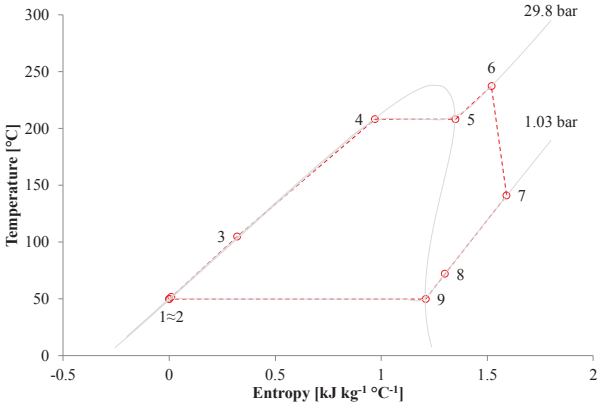

Figure 2. Saturation curve of cyclopentane in a $T-s$ diagram, showing the thermodynamic cycle state points of the organic Rankine cycle system.

3. STATE SPACE MODEL

The transient performance of ORC power systems is primarily driven by the thermal inertia of the heat exchangers. Figure 3 illustrates the discretized model utilized for the once-through boiler and the recuperator. The model features a 1D flow model for the hot side (top) and cold side (bottom), and the 1D thermal model for the tube walls (middle). A counter-flow configuration and uniform pressure distribution are assumed. The tube metal wall is modelled by a 1D dynamic

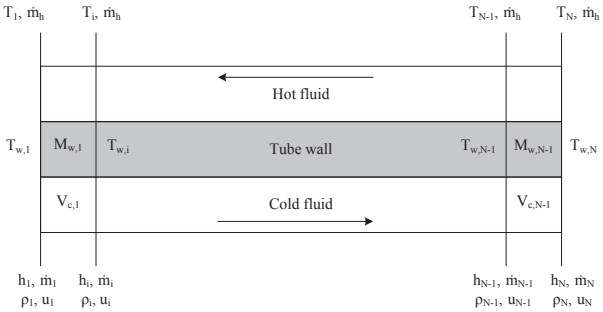

Figure 3. Heat exchanger discretized model.

heat balance equation, which for the i-cell can be written as

$$M_{\mathrm{w,i}} c_{\mathrm{w}} \frac{d\bar{T}_{\mathrm{w,i}}}{dt} = \dot{q}_{\mathrm{h}} - \dot{q}_{\mathrm{c}} \,, \tag{1}$$

where $M_{\mathrm{w,i}}$ and c_{w} are the mass and the heat capacity of the metal wall, and $\bar{T}_{\mathrm{w,i}}$ is the wall temperature at the i-volume, calculated as the arithmetic average between the temperatures at the inner and outer node. The variable $\dot{q}_{\mathrm{h}}$ is the heat provided by the hot stream and $\dot{q}_{\mathrm{c}}$ is the heat transferred to the cold side. The flow model for the cold side contains one-dimensional dynamic mass and energy balance equations, which can be expressed as

$$V_{\mathrm{c,i}} \frac{d(\bar{u}_{\mathrm{i}} \bar{\rho}_{\mathrm{c,i}})}{dt} = \dot{m}_{\mathrm{i}} h_{\mathrm{i}} - \dot{m}_{\mathrm{i+1}} h_{\mathrm{i+1}} + \dot{q}_{\mathrm{c}} \,, \tag{2}$$

$$V_{\mathrm{c,i}} \frac{d\bar{\rho}_{\mathrm{c,i}}}{dt} = \dot{m}_{\mathrm{i}} - \dot{m}_{\mathrm{i+1}} \,, \tag{3}$$

where $\dot{m}_{\mathrm{i}}$ and h_{i} represent the mass flow and the enthalpy at the i-node. The variables $\bar{u}_{\mathrm{c,i}}$ and $\bar{\rho}_{\mathrm{c,i}}$ are the internal specific energy and the density of the volume $V_{\mathrm{c,i}}$ calculated as arithmetic average between the values at the inner and outer node. In light of the relatively small variations with time of the thermodynamic properties on the gas side, steady state mass and energy balances are considered (see Equation 4).

$$\dot{q}_{\mathrm{h}} = c_{\mathrm{p,h}} \dot{m}_{\mathrm{h}} (T_{\mathrm{i+1}} - T_{\mathrm{i}}) \,. \tag{4}$$

Owing to their relatively small contributions, the thermal resistance in the radial direction and thermal diffusion in the axial direction are neglected. For the once-through boiler and the recuperator the heat transfer coefficient between the hot and the outer pipe surface is much lower than the one be-

tween the inner pipe surface and the ORC working fluid flow. Therefore, the overall heat transfer is essentially dependent on the hot side only, and the working fluid temperature is always close to the inner surface temperature of the pipe.

The heat transfer coefficient at the interface between the hot and the metal wall, in off-design conditions, is evaluated with the relation (Incropera, DeWitt, Bergman, & Lavine, 2007)

$$U = U_{\text{des}} \left(\frac{\dot{m}}{\dot{m}_{\text{des}}} \right)^{\gamma} , \tag{5}$$

where U is the heat transfer coefficient and the subscript "des" refers to the value at nominal operating conditions. The exponent γ, taken equal to 0.6, is the exponent of the Reynolds number in the heat transfer correlation. The thermal interaction between the wall and the cold stream is described by specifying a sufficiently high constant heat transfer coefficient, so that the fluid temperature is close to the wall temperature, and the overall result is dominated by the hot side heat transfer.

For the turbine the Stodola's cone law, expressing the relation between the pressure at the inlet and the outlet of the expander with the mass flow rate and the turbine inlet temperature is applied (Stodola, 1922). To predict the turbines off-design performance, the correlation relating the isentropic efficiency and the non-dimensional flow coefficient proposed by (Schobeiri, 2005) is utilized.

The isentropic efficiency of the pump in part-load is derived using the methodology proposed by (Veres, 1994), while the part-load characteristic of the electric generator is modelled using the equation suggested by (Haglind & Elmegaard, 2009).

Table 1 lists the parameters employed to parametrize the state space model of the ORC turbogenerator. The condensing pressure of the working fluid is fixed to 1.03 bar, corresponding to a temperature of 50 °C, so as to avoid inward air leakage into the condenser. The weight, volume and UA-values of the once-through boiler and the recuperator are obtained using an in-house simulation tool (Pierobon, Casati, Casella, Haglind, & Colonna, 2014), which has been extensively validated with public domain data.

Table 1. Design-point variables utilized to parametrize the state space model of the organic Rankine cycle system.

Component	Parameters
Gas turbine	
Exhaust temperature t_{10}	$379.2\,^{\circ}C$
Exhaust mass flow $\dot{m}_{10}$	$91.5\,kg\,s^{-1}$
Once-through boiler	
Volume (cold side)	$4\,m^3$
Weight (metal walls)	$50\,ton$
UA-value	$400\,kW\,K^{-1}$
Recuperator	
Volume (cold side)	$2\,m^3$
Weight (metal walls)	$5\,ton$
UA-value	$209.6\,kW\,K^{-1}$
Turbine	
Stodola constant	$30.4\,kg\,s^{-1}\,K^{0.5}\,bar^{-1}$
Isentropic efficiency	0.80
Electric generator efficiency	0.98
Pump	
Delivery pressure p_2	$29.8\,bar$
Inlet pressure p_1	$1.03\,bar$
Isentropic efficiency	0.72

4. UNSCENTED KALMAN FILTER ALGORITHM

In this section we will present the algorithm for the UKF for a general non-linear system. Let the system be represented by the following general non-linear discrete time equations

$$x_k = f(x_{k-1}, v_{k-1}, u_{k-1}) , \tag{6}$$

$$y_k = h(x_k, n_k, u_k) , \tag{7}$$

where $x \in \mathbb{R}^{n_x}$ is the system state, $v \in \mathbb{R}^{n_v}$ the process noise, $n \in \mathbb{R}^{n_n}$ the observation noise, u the input and y the noisy observation of the system.

The UKF algorithm is presented in the following (Julier & Uhlmann, 1997), (Wan & Van Der Merwe, 2000). Let the system be represented by (6) and (7). An augmented state at time instant k is defined

$$x_k^a \triangleq \begin{bmatrix} x_k \\ v_k \\ n_k \end{bmatrix} .$$

The augmented state dimension is,

$$N = n_x + n_v + n_n. \tag{8}$$

Similarly, the augmented state covariance matrix is built from the covariance matrices of x, v and n according to

$$P^a \triangleq \begin{bmatrix} P_x & 0 & 0 \\ 0 & P_v & 0 \\ 0 & 0 & P_n \end{bmatrix} ,$$

where P_v and P_n are the process and observation noise covariance matrices. Note that the augmented state is needed for non-additive noise; for additive noise the original state vector is sufficient.

$Initialization\ at\ k = 0:$

$$\begin{aligned} \widehat{x}_0 &= E[x_0] , \quad P_{x_0} = E\left[(x_0 - \widehat{x}_0)(x_0 - \widehat{x}_0)^T \right] , \\ \widehat{x}_0^a &= E[x^a] = E[\widehat{x}_0 \quad 0 \quad 0]^T , \\ P_0^a &= E\left[(x_0^a - \widehat{x}_0^a)(x_0^a - \widehat{x}_0^a)^T \right] = \begin{bmatrix} P_x & 0 & 0 \\ 0 & P_v & 0 \\ 0 & 0 & P_n \end{bmatrix} , \end{aligned}$$

For $k = 1, 2, ...\infty$:

Generate Sigma-points
Calculate $2N + 1$ sigma-points based on the present state covariance:

$$\mathbf{X}^a_{i,k-1} \begin{cases} \triangleq \widehat{x}^a_{k-1}, & i = 0 \\ \triangleq \widehat{x}^a_{k-1} + \gamma \mathbf{S}_i, & i = 1, ..., N \\ \triangleq \widehat{x}^a_{k-1} - \gamma \mathbf{S}_i, & i = N+1, ..., 2N \end{cases}, \quad (9)$$

where $\mathbf{S}_i$ is the ith column of the matrix,

$$S = \sqrt{P^a_{k-1}}.$$

In (9) γ is a scaling parameter

$$\gamma = \sqrt{N + \lambda}, \quad \lambda = \alpha^2(N + \kappa) - N \, ,$$

where α and κ are tuning parameters. We must choose $\kappa \geq 0$, to guarantee the semi-positive definiteness of the covariance matrix, a good default choice is $\kappa = 0$. The parameter α, $0 \leq \alpha \leq 1$, controls the size of the sigma-point distribution and it should ideally be a small number.

The ith sigma point (augmented) is the ith column of the sigma point matrix,

$$\mathbf{X}^a_{i,k-1} = \begin{bmatrix} \mathbf{X}^x_{i,k-1} \\ \mathbf{X}^v_{i,k-1} \\ \mathbf{X}^n_{i,k-1} \end{bmatrix} ,$$

where the superscripts x, v and n refer to a partition conformal to the dimensions of the state, process noise and measurement noise respectively.

Time-update equations
Transform the sigma points through the state-update function,

$$\mathbf{X}^x_{i,k/k-1} = f\left(\mathbf{X}^x_{i,k-1}, \mathbf{X}^v_{i,k-1}, u_{k-1}\right), \; i = 0, 1, ..., 2N \, .$$

Calculate the *a priori* state estimate and *a priori* covariance,

$$\begin{aligned} \widehat{x}^-_k &= \sum_{i=0}^{2N} \left(w^{(i)}_m \mathbf{X}^x_{i,k/k-1} \right) , \\ P^-_{x_k} &= \sum_{i=0}^{2N} w^{(i)}_c \left(\mathbf{X}^x_{i,k/k-1} - \widehat{x}^-_k \right) \left(\mathbf{X}^x_{i,k/k-1} - \widehat{x}^-_k \right)^T . \end{aligned}$$

The weights $w^{(i)}_m$ and $w^{(i)}_c$ are defined as,

$$\begin{aligned} w^{(0)}_m &= \frac{\lambda}{N + \lambda}, \;\; i = 0, \\ w^{(0)}_c &= \frac{\lambda}{N + \lambda} + (1 - \alpha^2 + \beta), \;\; i = 0, \\ w^{(i)}_m &= w^{(i)}_c = \frac{1}{2(N + \lambda)}, \;\; i = 1, ..., 2N, \end{aligned}$$

where β is a non-negative weighting parameter introduced to affect the weighting of the $zero$th sigma-point for the calculation of the covariance. This parameter (β) can be used to incorporate knowledge of the higher order moments of the distribution. For a Gaussian prior a typical choice is $\beta = 2$, as suggested by (Wan & Van Der Merwe, 2000).

Measurement-update equations
Transform the sigma points through the measurement-update function,

$$\mathbf{Y}_{i,k/k-1} = h\left(\mathbf{X}^x_{i,k/k-1}, \mathbf{X}^n_{k-1}, u_k\right), \; i = 0, 1, ..., 2N \, ,$$

and the mean and covariance of the measurement vector is calculated,

$$\begin{aligned} \widehat{y^-_k} &= \sum_{i=0}^{2N} w^{(i)}_m \mathbf{Y}_{i,k/k-1} \, , \\ P_{\overline{y}_k} &= \sum_{i=0}^{2N} w^{(i)}_c \left(\mathbf{Y}_{i,k/k-1} - \widehat{y^-_k} \right) \left(\mathbf{Y}_{i,k/k-1} - \widehat{y^-_k} \right)^T . \end{aligned}$$

The cross covariance is calculated according to

$$P_{x_k y_k} = \sum_{i=0}^{2N} w^{(i)}_c \left(\mathbf{X}^x_{i,k/k-1} - \widehat{x^-_k} \right) \left(\mathbf{Y}_{i,k/k-1} - \widehat{y^-_k} \right)^T .$$

The Kalman gain is given by,

$$K_k = P_{x_k y_k} P^{-1}_{\overline{y}_k},$$

and the UKF estimate and its covariance are computed from the standard Kalman update equations,

$$\widehat{x}_k = \widehat{x^-_k} + K_k \left(y_k - \widehat{y^-_k} \right),$$

$$P_{x_k} = P^-_{x_k} - K_k P_{\overline{y}_k} K^T_k .$$

5. SIMULATION RESULTS

In this section we present the simulation results derived by applying the UKF (see Section 4) on the ORC model described in Section 3 and parametrized according to Table 1. A static model of the gas turbine is included in the form of static functions to simulate the exhaust gas temperature and mass flow of the engine, *i.e.* the temperature and mass flow at node 10 in Figure 1. The static model serves as input to the ORC model and it is specified in terms of gas turbine load set-point. The ORC model was implemented on the form (6)–(7). The state of the fluid at each node from 1 to 8 (see Figure 1), is characterized by three state variables; mass flow $\mathbf{x}_{\dot{m}}$, density $\mathbf{x}_d$ and temperature $\mathbf{x}_T$, thus $\mathbf{x} = [\mathbf{x}^\top_T \; \mathbf{x}^\top_{\dot{m}} \; \mathbf{x}^\top_d]^\top$. The once-through boiler was discretized into 10 volumes with input and output at node 3 and 6, respectively (see Figure 2). All the state variables, *i.e.* mass flow, density and temperature of cyclopentane, are assumed to be measurable at all the nodes, *i.e.* 1 to 8, except 3 and 4 which are inside the device. The states

across the heat exchanger are not measurable. By taking into consideration the assumptions described in Sections 2 and 3, we have in total 45 states of which 18 are assumed to be measurable and 27 are not measurable and are estimated by using the UKF. Accordingly, $n_x = 45$, $n_v = 45$ and $n_n = 18$ as in (8). Additive process and measurement noise was assumed to be Gaussian with zero mean and covariance.

$$\begin{cases} P_v = & \text{diag}\{v_T\mathbf{I},\ v_d\mathbf{I},\ v_{\dot{m}}\mathbf{I}\} \\ P_n = & \text{diag}\{w_T\mathbf{I},\ w_d\mathbf{I},\ w_{\dot{m}}\mathbf{I}\}\ , \end{cases} \tag{10}$$

In Equation 10 $v_T = v_d = 0.01$, $v_{\dot{m}} = 1\times10^{-5}$, $w_T = w_d = w_{\dot{m}} = 0.1$, with identity matrices of appropriate dimensions according to the number of states and measurements. It is thus assumed that the observation noise is considerably larger than the process noise, and this case is considered to validate the robustness of the UKF with respect to noise. The parameters for the UKF where chosen as $\alpha = 1$, $\beta = 2$ and $\kappa = 0$. The simulation was run for $t \in [1, 400]$ seconds in steps of 1 second, where an abrupt change in the gas turbine load from 100% to 90% occurred at $t = 50$ seconds. The initial values where selected as

$$\begin{cases} \mathbf{x}_T(t_0) = & [323.1\ 324.9\ 377.6\ 392.1 \\ & 406.3\ 420.7\ 435\ 449.6\ 464.5\ 479.3 \\ & 481.1\ 481.1\ 507.4\ 410.9\ 340.9]^\top \\ \mathbf{x}_{\dot{m}}(t_0) = & 44.4\mathbf{I}_{15\times1} \\ \mathbf{x}_d(t_0) = & [714.9\ 716.5\ 658.9\ 641.2 \\ & 622.7\ 602.5\ 580.5\ 555\ 523.9\ 481.5 \\ & 211.8\ 111.2\ 71.2\ 2.7\ 2.7]^\top . \end{cases} \tag{11}$$

The simulation results for the scenario described above are shown in Figures 4–6(b). Figure 4 illustrates the temperature measurements with noise, the real and the UKF estimated temperatures at the inlet of the once-through boiler. Given the magnitude of the measurement noise, it is demonstrated that the UKF is capable of estimating the real temperature. Figure 5 shows the real and the UKF estimated temperatures in an intermediate section (fifth cell) of the heat exchanger where the UKF attempts to evaluate the real temperature with no measurements available. Figures 6(a) and 6(b) show the real and UKF estimated temperature distribution over the length of the once-through boiler at $t = 40$ and $t = 200$ seconds. To be noted that the temperature distribution is similar to that occurring between nodes 3 and 6 in Figure 2. Consequently, we can conclude that the UKF can reliably reconstruct the internal temperature distribution with no measurements available. Thus it has been shown that the UKF is applicable to monitor the condition of the heat exchanger.

To test the robustness of the UKF with respect to initial conditions a new simulation was performed where the initial temperature estimates were different from the actual values. The

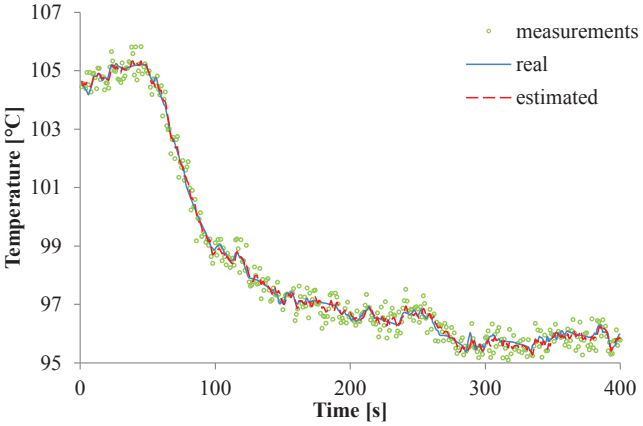

Figure 4. Real, estimated and measured temperature profiles at the inlet of the once-through boiler.

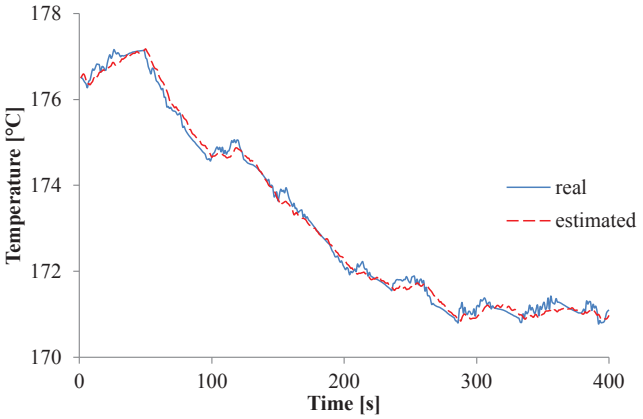

Figure 5. Real and estimated temperature profiles at an intermediate section of the once-through boiler.

new simulation was carried out so that all the first temperature estimates to the UKF are 3°C higher than the actual initial values. As the purpose of this simulation was to test the robustness with respect to initial state estimation, no change in the gas turbine load is applied. Otherwise the simulation set-up is similar to the previous case. The new results are shown in Figures 7–8. Figure 7 reports the temperature measurements with noise, the real and the UKF estimated temperatures at the inlet of the heat exchanger. Given the magnitude of the erroneous initial condition, it is demonstrated that the UKF estimate of the temperature is able to converge to the real temperature within the first time step. Figure 8 shows the real and the estimated temperatures at an intermediate section (fifth cell) of the once-through boiler. It can be observed that the UKF projection converged to the real temperature despite the lack of available measurements. Moreover, the estimate converged to the real temperature within approximately 100 seconds which is a reasonable time frame for this type of system.

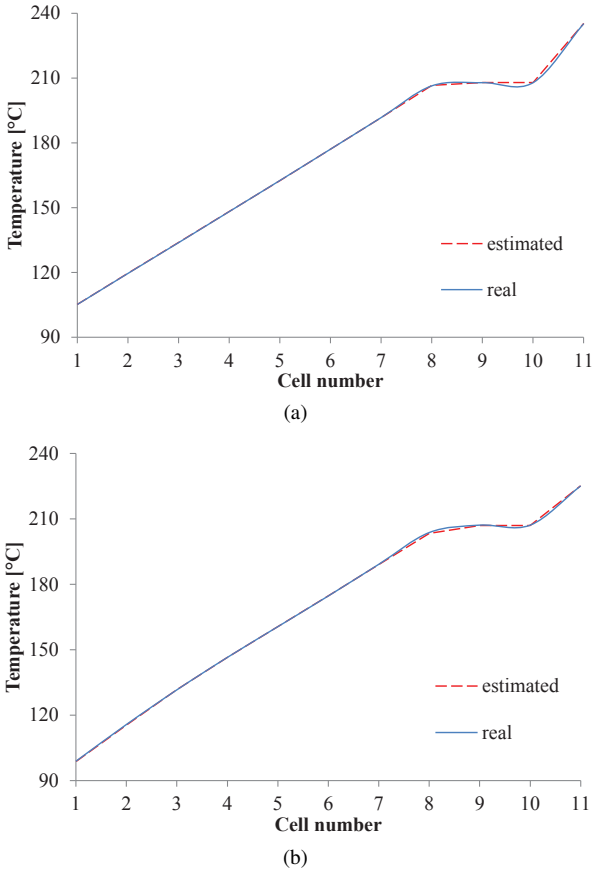

Figure 6. Real and estimated temperature distribution along the cells of the once-through boiler. 6(a) at time $t = 40$ seconds and 6(b) at time $t = 200$ seconds.

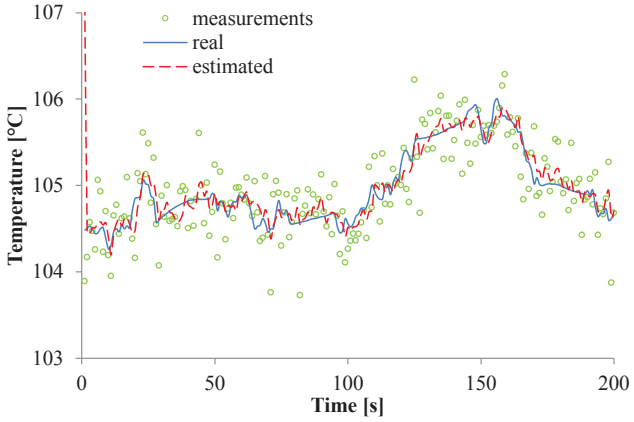

Figure 7. Real, estimated and measured temperature profiles at the inlet of the once-through boiler. The initial estimated temperature is 3°C higher than the real temperature.

6. CONCLUSION

This paper analysed the use of the Unscented Kalman Filter to predict the temperature profile inside a once-through boiler serving an organic Rankine cycle turbogenerator. Simulation results demonstrate the stability of the UKF, even with aggressive additive Gaussian noise profiles for process and measurements, and for a heat exchanger discretized into a relatively large number of volumes with unmeasured states. Furthermore, it was observed that the estimated temperature converged to the real values in a reasonable time frame when relatively reasonable deviations in the initial guess for all nodes were applied.

Future work will focus on applying the UKF to the combined cycle unit consisting of the gas turbine and the ORC turbogenerator. The estimation results will be embedded in the control algorithm of the integrated system. Further work will be directed towards the implementation of UKF with constraints on the state variables applied to this integrated system.

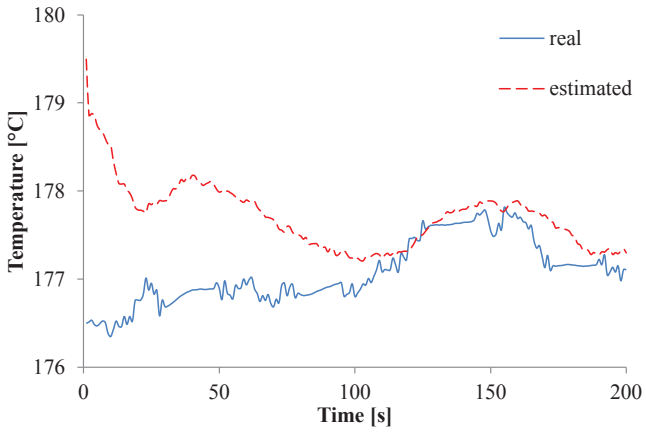

Figure 8. Real and estimated temperature profiles at an intermediate section of the once-through boiler. The initial estimated temperature is 3°C higher than the real temperature.

ACKNOWLEDGEMENT

The funding from the Norwegian Research Council through Petromaks with project number 203404/E30, which is lead by Teknova, is acknowledged.

REFERENCES

Bolland, O., Forde, M., & Hånde, B. (1996). Air bottoming cycle: use of gas turbine waste heat for power generation. *Journal of engineering for gas turbines and power*, *118*, 359-368.

Del Turco, P., Asti, A., Del Greco, A., Bacci, A., Landi, G., & Seghi, G. (2011, June). The ORegen waste heat recovery cycle: Reducing the CO_2 footprint by means of overall cycle efficiency improvement. In *Proceedings of ASME Turbo Expo 2011* (pp. 547–556). Vancouver,

Canada.

Haglind, F., & Elmegaard, B. (2009). Methodologies for predicting the part-load performance of aero-derivative gas turbines. *Energy*, *34*(10), 1484 - 1492.

Incropera, F. P., DeWitt, D. P., Bergman, T. L., & Lavine, A. S. (2007). *Fundamentals of heat and mass transfer* (6th ed.). Jefferson City, United States of America: John Wiley & Sons, Inc. (ISBN: 9780470501979)

Jonsson, G., & Palsson, O. P. (1994). An application of extended kalman filtering to heat exchanger models. *Journal of dynamic systems, measurement, and control*, *116*(2), 257–264.

Jonsson, G. R., Lalot, S., Palsson, O. P., & Desmet, B. (2007). Use of extended kalman filtering in detecting fouling in heat exchangers. *International journal of heat and mass transfer*, *50*(13), 2643–2655.

Julier, S. J., & Uhlmann, J. K. (1997). New extension of the kalman filter to nonlinear systems. In *Proceedings of signal processing, sensor fusion, and target recognition VI* (pp. 182–193).

Kandepu, R., Foss, B., & Imsland, L. (2008). Applying the unscented kalman filter for nonlinear state estimation. *Journal of Process Control*, *18*(7), 753–768.

Kloster, P. (1999, 7-9 September). Energy optimization on offshore installations with emphasis on offshore combined cycle plants. In *Offshore europe conference* (p. 1-9). Aberdeen, Great Britain: Society of Petroleum Engineers.

Loparo, K., Buchner, M., & Vasudeva, K. (1991). Leak detection in an experimental heat exchanger process: a multiple model approach. *Automatic Control, IEEE Transactions on*, *36*(2), 167–177.

Nguyen, T.-V., Pierobon, L., Elmegaard, B., Haglind, F., Breuhaus, P., & Voldsund, M. (2013). Exergetic assessment of energy systems on North Sea oil and gas platforms. *Energy*, *62*(0), 23 - 36.

Pierobon, L., Casati, E., Casella, F., Haglind, F., & Colonna, P. (2014). Design methodology for flexible energy conversion systems accounting for dynamic performance. *Energy*, *68*, 667–679.

Pierobon, L., Haglind, F., Kandepu, R., Fermi, A., & Rossetti, N. (2013, November). Technologies for waste heat recovery in off-shore applications. In *Proceedings of ASME 2013 International Mechanical Engineering Congress & Exposition* (p. 1-10). San Diego, California.

Pierobon, L., Nguyen, T.-V., Larsen, U., Haglind, F., & Elmegaard, B. (2013). Multi-objective optimization of organic Rankine cycles for waste heat recovery: Application in an offshore platform. *Energy*, *58*, 538–549.

Quoilin, S., Broek, M. V. D., Declaye, S., Dewallef, P., & Lemort, V. (2013). Techno-economic survey of organic Rankine cycle (ORC) systems. *Renewable and Sustainable Energy Reviews*, *22*, 168–186.

Schobeiri, M. (2005). *Turbomachinery flow physics and dynamic performance*. Berlin, Germany: Springer Berlin. (ISBN: 9783540223689)

Stodola, A. (1922). *Dampf- und gasturbinen: Mit einem anhang über die aussichten der wärmekraftmaschinen*. Berlin, Germany: Springer Berlin. (ISBN: 7352997563)

Veres, J. P. (1994). *Centrifugal and axial pump design and off-design performance prediction* (Tech. Rep.). Sunnyvale, United States of America: NASA. (Technical Memorandum 106745)

Wan, E. A., & Van Der Merwe, R. (2000). The unscented kalman filter for nonlinear estimation. In *Adaptive systems for signal processing, communications, and control symposium* (pp. 153–158).

BIOGRAPHIES

L. Pierobon is a PhD candidate at the Technical University of Denmark (DTU). He obtained his BSc and MSc degrees in Energy Engineering from University of Padova, Italy in 2008 and 2010, respectively. He is currently involved in the EOOS project financed by the Norwegian research council; the primary scope is to optimize the energy production in offshore platforms.

R. Schlanbusch received his BSc and MSc degrees in Space Technology from Narvik University College (NUC), Narvik, Norway, in 2005 and 2007 respectively, and PhD degree in Engineering Cybernetics from NTNU, Trondheim, Norway in 2012. He currently holds a position as senior researcher at Teknova, Norway, and a II position as associate professor at department of Technology, NUC, Norway.

R. Kandepu received his Masters in Control and Instrumentation from Indian Institute of Technology (IIT), Delhi, India in 2003. He received his PhD degree in Engineering Cybernetics from NTNU, Trondheim, Norway in 2007. He currently holds a position as senior researcher at Teknova, Norway.

F. Haglind received his MSc degree from Lund University, Sweden, in Mechanical Engineering in 1999 and his PhD degree from Cranfield University, UK, in Mechanical Engineering in 2005. Currently he holds a position as Associate Professor at Technical University of Denmark, Department of Mechanical Engineering. His primary research field is power plant engineering, with focus on low-temperature power cycles and gas turbines/combined cycles. He teaches in fundamental and applied engineering thermodynamics.